frontiers | Frontiers in Marine Science

TYPE Original Research
PUBLISHED 02 January 2026
DOI 10.3389/fmars.2025.1718186

OPEN ACCESS

EDITED BY
Jacopo Chiggiato,
National Research Council (CNR), Italy

REVIEWED BY
Milena Menna,
National Institute of Oceanography and Applied Geophysics (Italy), Italy
Javier Soto-Navarro,
University of Malaga, Spain
Dimitris Velaoras,
Hellenic Centre for Marine Research (HCMR), Greece

*CORRESPONDENCE
Elena Terzić
eterzic@irb.hr

RECEIVED 03 October 2025
REVISED 18 November 2025
ACCEPTED 25 November 2025
PUBLISHED 02 January 2026

CITATION
Terzić E and Vilibić I (2026) Twenty-first century thermohaline trends and abrupt shifts in the Ionian Sea. *Front. Mar. Sci.* 12:1718186. doi: 10.3389/fmars.2025.1718186

Twenty-first century thermohaline trends and abrupt shifts in the Ionian Sea

Elena Terzić[1]* and Ivica Vilibić[1,2]

[1]Ruđer Bošković Institute, Division for Marine and Environmental Research, Zagreb, Croatia, [2]Institute for Adriatic Crops and Karst Reclamation, Split, Croatia

Being centrally located within the basin and exhibiting internally driven quasi-decadal variability, the Ionian Sea serves as a pivotal conduit for water-mass exchange between the Western and Eastern Mediterranean. Using 23 years (2001–2024) of Argo float profiles, we quantify recent thermohaline changes across six sub-basins of the Ionian. Throughout the study period, pronounced warming and salinification were observed, occurring at rates much higher than during the 20th century. Between 2022 and 2024, the southern and south-eastern Ionian intermediate waters (300–1200 m) warmed by 0.7–1.8°C and their salinity increased by 0.24–0.40, with maxima near 700–1000 m, reflecting an abrupt shift in water-mass properties. Concurrent ERA5 reanalysis reveals a pronounced negative winter heat-flux anomaly in 2021/2022, intensified wind stress, and elevated evaporation minus precipitation, all of which favored much pronounced convective mixing that transferred warm and saline waters to deeper layers. In parallel, anomalous intermediate-layer properties observed in the southern Adriatic during the same period suggest a broader, interconnected response of the Adriatic–Ionian system. Together, these processes may indicate a transition toward a warmer, more saline deep-Ionian state. If sustained, such a regime could weaken dense-water formation, alter the Mediterranean overturning circulation, and propagate anomalies westward into the Atlantic through the Gibraltar outflow.

KEYWORDS

Ionian Sea, Argo floats, thermohaline variability, Adriatic-Ionian Bimodal Oscillation - BiOS, dense water formation, Mediterranean overturning circulation, climate change, Eastern Mediterranean atmospheric variability

1 Introduction

The Ionian Sea is a region crucial for the exchange of key water masses across the Mediterranean Sea, connecting its western and eastern parts with the Adriatic and Aegean Seas (Berline et al., 2021). Its general circulation pattern consists of Atlantic Water (AW) traveling eastward toward the Levantine basin, increasing in both temperature and salinity along the way, where high evaporation favors the formation of Levantine Surface Water (LSW). Under winter cooling, this water eventually sinks, forming Levantine Intermediate

Water (LIW) in the Levantine Sea or Cretan Intermediate Water (CIW) in the southern Aegean Sea. At its deepest layers, the Eastern Mediterranean Deep Water (EMDW) originates either from the Adriatic or the Aegean Sea. The latter exerted its strongest influence after the Eastern Mediterranean Transient (EMT; Klein et al., 1999) in the 1990s, when much warmer and saltier deep waters spread across the basin, progressively homogenizing the layer between 3000 and 4000 m. This process led to an increase in heat storage that was twice as high as global estimates (Artale et al., 2018).

The Ionian surface circulation consists of a large gyre that alternates between cyclonic and anticyclonic regimes on a quasi-decadal scale due to the Bimodal Oscillating System (BiOS; Gačić et al., 2010). The anticyclonic circulation brings fresher, cooler Atlantic waters into the northern Ionian Sea and usually suppresses dense water formation in the Adriatic. Dense waters are generated both in the shallow northern Adriatic due to cold and dry bora winds (Raicich et al., 2013), and within the Southern Adriatic Pit through open-ocean convection (Gačić et al., 2002). These processes contribute to greater ventilation of the deepest layers of the Ionian and Eastern Mediterranean. Conversely, the cyclonic phase brings warmer, saltier LIW and thus enhances Adriatic dense water formation. Anticyclonic gyres of the Eastern Mediterranean also promote LIW sinking and affect its intermediate depth flow (Menna et al., 2021). One example is the Pelops gyre, located in the northeastern Ionian Sea, which is involved in the circulation and exchange of Levantine-origin surface and intermediate waters by advecting flow along western Greece toward the Ionian and Adriatic seas (Menna et al., 2021; Androulidakis et al., 2024).

The BiOS mechanism acts as a central driver of decadal variability in the Eastern Mediterranean, shaping circulation, deep-water formation, and biogeochemistry (Civitarese et al., 2023). Its influence extends across the entire basin, linking regional circulation changes to larger-scale processes ranging from water-mass propagation to ecosystem impacts. The Adriatic Deep Water (AdDW), formed in winter due to cooling and salinity buildup, feeds the deep thermohaline cell of the Eastern Mediterranean and unbalances the vorticity that, in turn, changes the circulation in the northern Ionian Sea from cyclonic to anticyclonic and vice versa. As a feedback, BiOS modulates the inflow of water masses towards the dense water sites and therefore directly influences the deep circulation and thermohaline properties of the Ionian-Adriatic thermohaline system (Gačić et al., 2010). Because Eastern Mediterranean intermediate and deep waters ultimately affect circulation across the Sicily Channel that brings LIW into the Western Mediterranean (Gačić et al., 2013), BiOS-driven variability in the east can reverberate throughout the whole Mediterranean. Changes in BiOS-driven circulation and associated salinity–temperature patterns also contribute to steric sea-level variability and broader water-mass redistribution, impacting long-term climate and oceanographic trends (Borile et al., 2025). By altering the advection of different water masses, BiOS influences not only plankton phenology (Lavigne et al., 2018), but also its community structure, as well as higher trophic levels, including zooplankton (Batistić et al., 2014), fish populations (Patti et al., 2025), especially in the Adriatic region (Civitarese et al., 2010, Civitarese et al., 2023). From 2001 to 2011, AdDW strongly influenced central and western Ionian waters (Budillon et al., 2010), but this impact weakened between 2011 and 2018 as ventilation decreased (Li and Tanhua, 2020). Observations from recent decades reveal an increasing trend of warming and salinification in the Eastern Mediterranean (Skliris et al., 2024; Zodiatis et al., 2023). Specifically, in 2024, the Ionian Sea reached the warmest conditions of the past four decades, with mean summer surface temperatures exceeding 28 °C and trends of up to 0.59 °C per decade between 1982 and 2024 (Androulidakis et al., 2024). Changes in upper thermohaline circulation in the Eastern Mediterranean may also create favorable conditions for dense water formation in the Aegean Sea through salinity preconditioning (Velaoras et al., 2014; Potiris et al., 2024a, Potiris et al., 2024b). Similar changes have been observed in the southern Adriatic (Terzić et al., 2025a). Both processes could lead to drastic shifts in EMDW, which—when formed in the Adriatic—has so far supplied cooler, more oxygenated waters to the Ionian Sea (Budillon et al., 2010).

In this study, we analyze 23 years (2001–2024) of Argo float observations to quantify thermohaline variability across six sub-basins of the Ionian Sea. We place particular emphasis on the abrupt warming and salinification observed between 2022 and 2024, investigate the role of surface forcing anomalies in driving these changes, and discuss their implications for deep-water formation and the Mediterranean overturning circulation. To provide a coherent framework for these objectives, we structured the analysis in three complementary stages: (i) the entire 2001–2024 record is examined qualitatively to capture the long-term evolution and to illustrate early signals of change despite the sparser pre-2012 sampling. (ii) Quantitative trend estimates are then derived for 2012–2022, a period characterized by quasi-linear increases in temperature and salinity and by the most homogeneous spatial coverage of Argo profiles. (iii) Finally, we isolate the 2022–2024 interval—when an abrupt thermohaline shift becomes evident—to compare post-and pre-event conditions (2024 vs 2022) and to relate these differences to contemporaneous anomalies in heat, water, and momentum exchanges. This tiered approach ensures that the early data are retained for context while statistical inferences rely on the most robust portion of the record, thus directly addressing the study's main question: how recent atmospheric forcing anomalies have reshaped the thermohaline structure of the Ionian Sea within the broader multi-decadal evolution.

2 Materials and methods

2.1 Argo data

Argo profiling floats data were downloaded for the Ionian Sea from the Euro-ARGO ERIC database, as shown in Figure 1. Parameters of temperature (T [$^{\circ}C$]) and practical salinity (S [-]) were used, from which values of the potential density anomaly referenced to the surface (PDA [kgm^{-3}]) were obtained using the TEOS-10 standards (https://www.teos-10.org). Data were

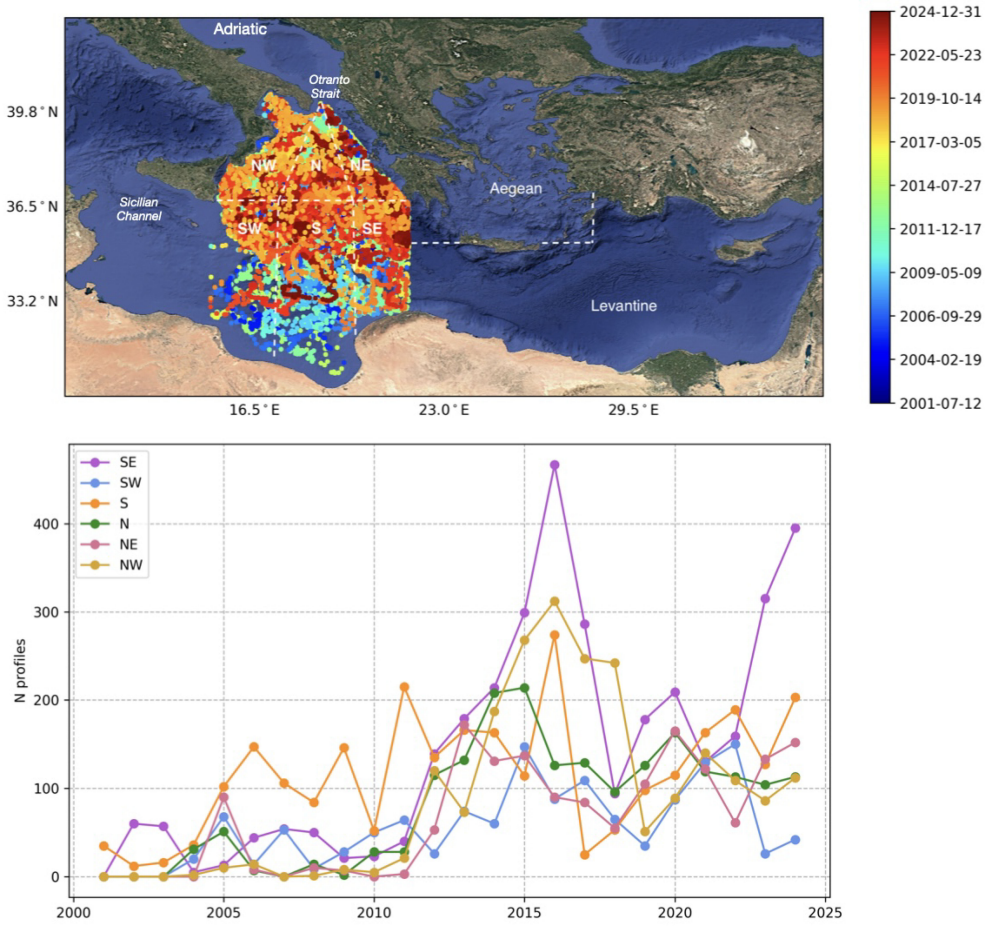

FIGURE 1
The Eastern Mediterranean Sea geography, with a color-coded time span of the Argo profiles used in the research and marked regions over which the analyses have been carried out: the Ionian Sea, the Aegean Sea and the Levantine basin (image background from @Google Maps). The Ionian Sea is sub-divided into 6 regions, which are delineated with the white dashed lines: the north-western (NW), northern (N), north-eastern (NE), south-western (SW), southern (S) and south-eastern (SE) basins. Bottom: the annual number of Argo profiles per basin.

downloaded through the ArgoPy data fetcher (https://pypi.org/project/argopy/), last accessed on 17 February 2025. The temporal range of acquired profiles is between 2001 and 2024, following 98 active floats carrying out 13.153 vertical profiles in total. Only solid quality control (QC) profiles were chosen, i.e., QC = 1 ("good") and QC = 2 ("probably good") in delayed, but also real-time mode in order to include profiles from still active floats. 91.6% profiles had a QC = 1 (good) for *T* and 78.3 % for *S*. Each Argo profiling float is identified by a unique World Meteorological Organization (WMO) number, which is used in global databases to track float trajectories, metadata, and profile archives. Several additional conditions were established with the aim of removing inadequate profiles for analysis. For example, the minimum depth of each profile had to be 500 m and the first depth quota had to be a positive number. In addition, the salinity values had to be greater than 30, as some low values were observed after a visual inspection of the data set and labeled as bad data. Only acquisitions in ascending mode were taken into consideration, and an additional visual inspection of each float's time series enabled to discard the ones with only a handful of profiles over time with big temporal gaps between two subsequent acquisitions.

To resolve spatial variability within the Ionian Sea while maintaining statistical robustness, the basin was divided into six sub-basins: north-western (NW), northern (N), north-eastern (NE), south-western (SW), southern (S), and south-eastern (SE) sectors, Figure 1. The subdivision was designed according to two complementary criteria:

1. Data-coverage criterion: the Argo profile density is quasi-homogeneous across these six areas, ensuring that each sector contains a comparable number of profiles throughout the 2001–2024 record (62, 62, 51, 70, 57 and 51 floats were profiling in the NW, N, NE, SW, S and SE sectors, respectively). Increasing the number of sectors would have resulted in spatially fragmented or sparsely populated domains, reducing the statistical reliability of the trend estimates.
2. Dynamical criterion: the boundaries were drawn following the main circulation features of the Ionian Sea, which vary

under the BiOS regime (e.g., Pinardi et al., 2019; Menna et al., 2019, Menna et al., 2021; Estournel et al., 2021). In particular, the Mid-Ionian Jet (MIJ; 36–36.5°N) was used as a guiding reference separating the northern and southern regimes. The northern Ionian was further divided into three dynamically distinct sectors:

- the NE sector, dominated by a northwestward flow toward the Strait of Otranto and partially deflected westward;
- the N sector, located near the BiOS vorticity maximum and sensitive to its regime changes; and
- the NW sector, where southwestward circulation prevails and where the deep Adriatic outflow interacts with Ionian intermediate layers.

The southern Ionian was likewise divided into three sectors (S, SE, SW) to account for the dominant inflow of Atlantic Water and Levantine Intermediate Water and to capture the contrasting properties between the Pelops Gyre region (SE) and the western and central Ionian basins. This physically informed yet statistically balanced subdivision allows us to examine thermohaline variability across regions representing distinct dynamical environments within the Ionian Sea.

2.2 Atmospheric data

The total heat flux and its components (latent, sensible, shortwave and longwave fluxes), total precipitation and evaporation, wind speed components, and the drag coefficient for momentum transfer (which was needed to obtain wind stress) were taken from the ERA5 hourly reanalysis (Hersbach et al., 2023), last accessed on 26 June 2025. Data were averaged over the Levantine basin, Ionian and Aegean seas (latitude ranges 33-36°, 33-36°, 35-41° and longitude ranges 22-33°, 12-21°, 21-28°, respectively), in order to quantify their variability between different Eastern Mediterranean basins. Daily and seasonal anomalies were estimated with respect to the daily climatology of 1980-2010.

2.3 Trend estimation and statistical analysis

To quantify long-term thermohaline changes, trends were computed separately for each Ionian sub-basin and standard depth level using the monthly-median time series derived from Argo profiles. First, all individual profiles within a given sector and depth were aggregated into monthly median values. Before trend estimation, the seasonal cycle was removed from each time series by subtracting a harmonic fit containing both the 12- and 6-month components, following Argo-based climate analyses (Chen and Wang, 2016; Gouretski, 2018). This procedure effectively isolates the interannual variability and longer-term signals. Linear trends were then calculated using ordinary least-squares regression of the depersonalized monthly anomalies against time, yielding the slope (rate of change), intercept, and statistical significance. Unless otherwise stated, we consider trends statistically significant when $p<0.01$. To examine recent abrupt changes, the 2022–2024 interval was excluded from linear regressions and analyzed separately by computing annual-median differences between 2024 and 2022 for each sector and depth. This approach ensures that quasi-linear behavior during 2012–2022 is evaluated independently of the recent step-like shift, while retaining all earlier data for qualitative context.

Time series were computed by aggregating all available data per each 100 m, accounting for an additional layer below of 20 m thickness. Float numbers per each layer (from 100 to 2000 m, with less floats at greater depths) varied between: from 60 to 32 for SE, from 54 to 26 for S, from 50 to 20 for SW, from 53 to 25 for NE, from 50 to 29 for N and from 49 to 18 for NW Ionian regions, respectively.

2.4 Sampling representativeness and coverage

To assess the potential influence of uneven sampling on the derived trends, we examined the spatial and temporal distribution of Argo profiles within each sub-basin (Figure 1). The northern portions of the southern sectors (SW, S, SE) are characterized by continuous coverage throughout the record, whereas the southernmost portions were more intensively sampled before 2011. This heterogeneity primarily reflects the historical evolution of the Argo network rather than systematic changes in water-mass properties. To minimize possible bias, all analyses were performed on monthly-median series, so that months with a greater number of high-frequency profiles (e.g., floats operating in the Pelops Gyre region) do not overweight the trend estimates. Consequently, the impact of different float cycling intervals or the presence of dedicated high-frequency missions is negligible once the data are aggregated to the monthly scale.

3 Results

3.1 Basin-wide float observations

To illustrate the temporal and vertical evolution of thermohaline properties within the Ionian Sea, we first analyzed two representative Argo floats that sampled the basin over multi-year trajectories. These floats were selected because they each traversed the Ionian Sea across its main zonal extent, one moving from west to east and the other from east to west, thus capturing contrasting circulation pathways and water-mass regimes. This approach serves two purposes: (i) to document the detailed thermohaline variability recorded along individual float paths, providing examples of the observed temperature–salinity changes, and (ii) to familiarize the reader with the underlying data structure and variability that form the basis for the subsequent statistical analyses of trends and 2024–2022 differences. The spatial trajectories color-coded in time and the corresponding Hovmöller diagrams are shown in Figures 2 and 3).

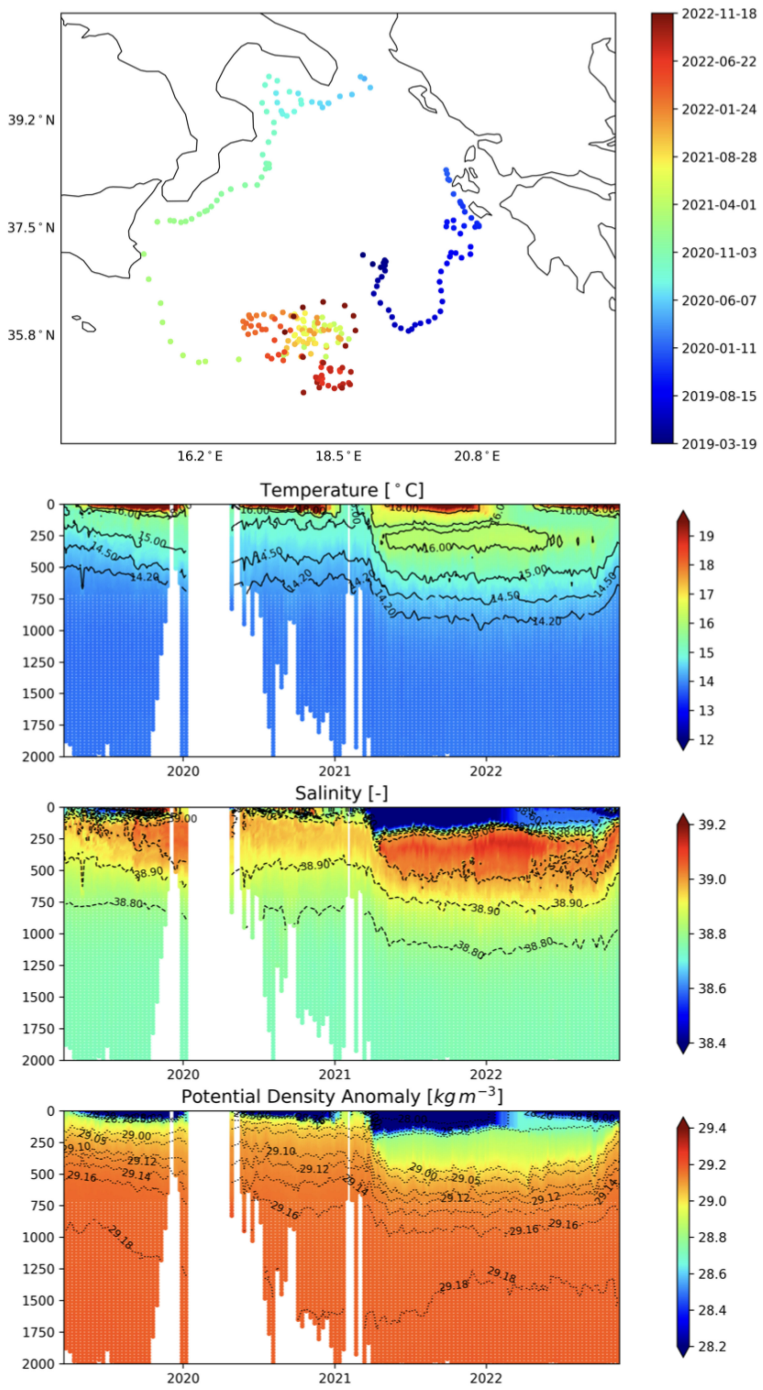

FIGURE 2
Top: trajectory of float WMO 6903262, color-coded by time. Below: Hovmöller diagrams for *T*, *S* and *PDA* for the same float. Profiles with maximum depths shallower than 500 m were excluded from the analysis.

The first example shows a float (WMO 693262) traveling counterclockwise from the eastern shores, first towards the Otranto Strait and then back south to the central southern Ionian (Figure 2). The Hovmöller diagram shows a noticeable difference around summer 2021 when floating in gyres in the S and SW Ionian: surface *S* drops below 38.3, as the float intercepts AW intrusion in the central Ionian Sea. Intermediate depths, between 200 and 500 m, have increased values of *T* around 16°C and *S* reaching over 39.1 until the end of the float sampling in November 2022. The central part, reached during summer 2021, delineates a clear front with warmer and saltier waters at intermediate depths flowing from CIW/LIW towards the central Ionian, creating a substantial vertical stratification towards the surface waters originating from the Atlantic.

The second example (WMO 6903788), deployed in the south-western Ionian (Figure 3), gradually travelled northward toward the

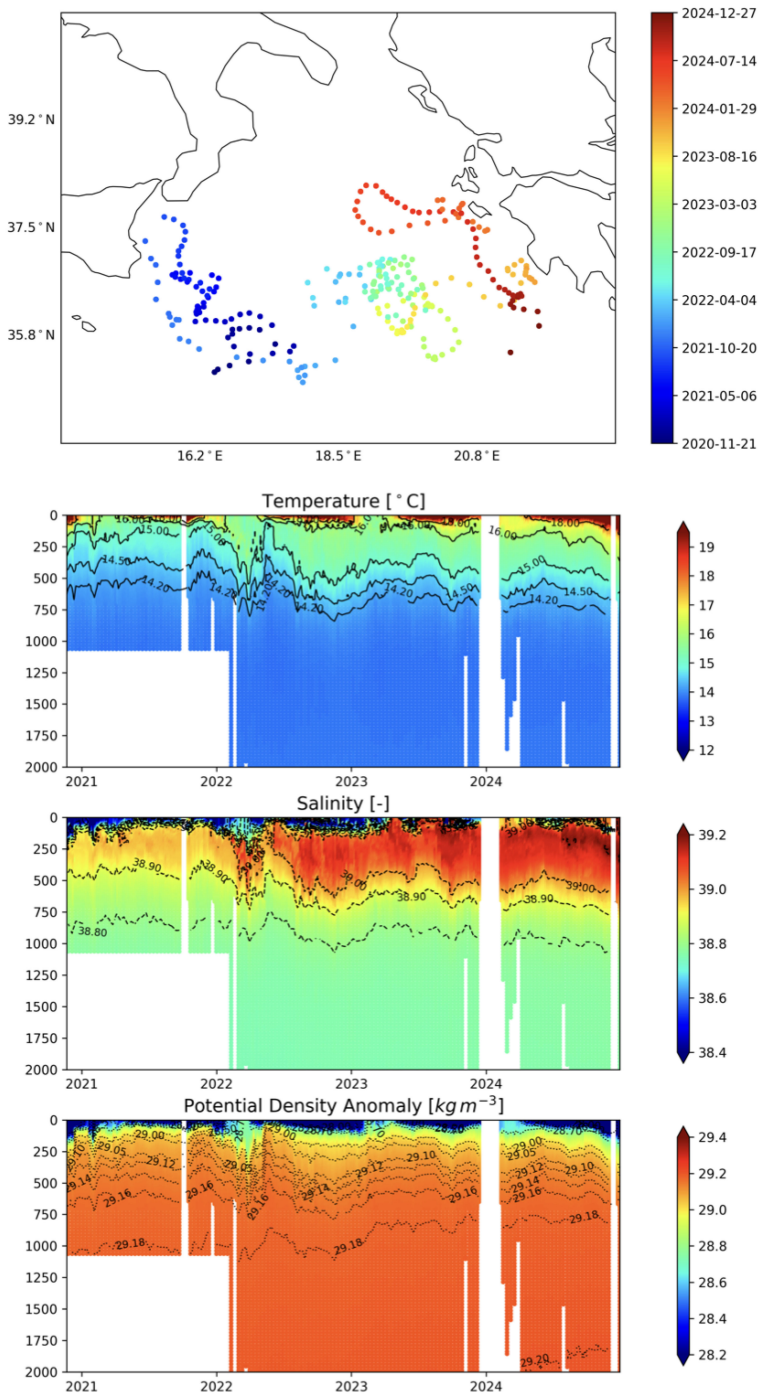

FIGURE 3
Top: trajectory of float WMO 6903788, color-coded by time. Below: Hovmöller diagrams for *T*, *S* and *PDA* for the same float. Profiles with maximum depths shallower than 500 m were excluded from the analysis.

north-eastern Sicilian coast before being advected southeastward toward the south-central Ionian. the float was entrained by the Mid-Ionian Jet (MIJ), which transported it eastward along the quasi-zonal pathway separating the northern and southern Ionian gyres. Along this trajectory, the float recorded the intrusion of warmer and saltier LIW waters between the southern parts of the N and NE Ionian sub-basins. Subsequently, it circulated within both cyclonic and anticyclonic gyres, moving toward the NE and finally the SE Ionian. The layers of warmer and saltier waters progressively thickened with time, the 38.9 halocline reaching depths up to 700 m and the 16°C thermocline expanding to 600 m. Lower surface salinities ($S < 38.6$) persisted until the end of the circular trajectory before the float began moving eastward again in January 2024.

3.2 Sub-basin trends and variability

The time series of floats at 500 m for *T* (Figure 4), *S* (Figure 5) and *PDA* (Figure 6), color coded by float, for each of the 6 Ionian regions, reveal trends of increasing *T* and *S* for the past two decades, since the beginning of measurements. Temperatures have increased between 0.5-1°C (N and NW Ionian) and 0.5-2.5°C in the SE Ionian since 2004, most notably since 2016, reaching values of up to 16°C in some parts of the sub-basin (Figure 6). Salinities also reveal increasing trends for all regions, most notably in the SE Ionian (with an increase of 0.2-0.5 in the last two decades), followed by the S Ionian (0.15-0.35 increase), while the NW, N, NE and SW Ionian increased by 0.1-0.2 (Figure 5). *PDA* seems to have stable values in the Northern (N, NW and NE) Ionian, oscillating around 29.15 kgm^{-3}, but showing a decreasing trend in the S and SE Ionian, illustrating the impact that the strong warming rate has had on density in recent years (Figure 6).

Furthermore, in the Supplementary material, Supplementary Figures S1 to Figures S12, display similar WMO color-coded time series for *T*, *S*, and *PDA* at 100 m, 1000 m, 1500 m and 2000 m. At 100 m, despite pronounced seasonal variability, temperatures in the SE Ionian reveal an accelerating warming trend, occasionally increasing from 15-16°C to 21-22°C during years in which the seasonal thermocline reached larger depths. Although the Argo record before 2012 is sparse, no comparable deep thermocline intrusions are evident in the existing profiles prior to 2016. In addition, this region recorded quite a strong temperature increase in 2023 and 2024. S Ionian temperature reveals an increase from 14–15 to 18°C and the other 4 regions showing an increase from 14–15 to 16-17°C (Supplementary Figure S1). Salinity has also had an increasing trend in all regions, occasionally resulting in values as high as 39.5 in the SE Ionian in 2020 and 2024, up to 39.2 in the S Ionian and maximum values of 39.1 in other regions. In contrast, no salinity above 39.0 was recorded in any basin before 2011 (Supplementary Figure S2). At greater depths, increases in *T* and *S* in the SE Ionian become more drastic, especially at 1000 m (Supplementary Figure S4-Supplementary Figure S6) and 1500 m (Supplementary Figures S7-Figures S9), resulting in an increase of more than 2°C in *T* at 1000 m (Supplementary Figure S4) and 1.5°C at 1500 m (Supplementary Figure S7) only since 2023, as evidenced by at least 4 different floats. The same holds for *S*, where the values jumped from 38.8 to 39.2 at 1000 m (Supplementary Figure S5) and from 38.75 to 38.85 at 1500 m (Supplementary Figure S8). *PDA* is dominated by the increase in *T*, which results in a drop from 29.18 kgm^{-3} to 29.07 kgm^{-3} at 1000 m (Supplementary Figure S6) and from 29.19 to 29.17 kgm^{-3} at 1500 m (Supplementary Figure S7). In fact, these jumps indicate an unprecedented deepening of the warm and salty surface waters into deep layers, presumably due to documented changes in the sources of water mass (see the discussion in Section 4). At 2000 m, in the SE Ionian *T* in the past year increased from 13.5 to 13.6°C (Supplementary Figure S10), *S* from 38.74 to 38.78 (Supplementary Figure S11) and *PDA* from 29.2 to 29.18 kgm^{-3} (Supplementary Figure S12).

The time series results can be aggregated and further corroborated in the form of linear trends in the decade between 2012-2022, before the appearance of abrupt jumps in both *T* and S. Since the data before 2012 are quite sparse, they were not used for the computation of trends. Warming rates in the SE Ionian reach up to 0.42-0.51°C/decade between 200 and 500 m (Figure 7a), with a maximum value at 400 m. The SE Ionian region is followed by the NE (rates between 0.40 and 0.50°C/decade 200–500 m) and N (0.37 and 0.41°C /decade for 200 and 300 m) Ionian regions. Salinity

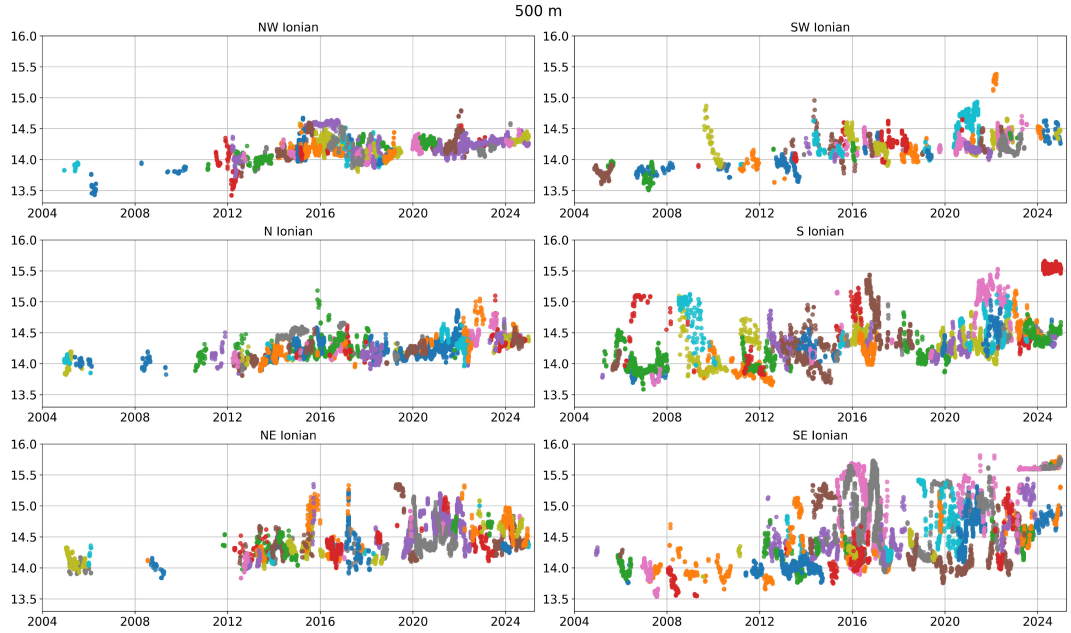

FIGURE 4
Time series for *T* at 500 m depth, each subplot for one of the 6 Ionian sub-basins. Each color represents a different float.

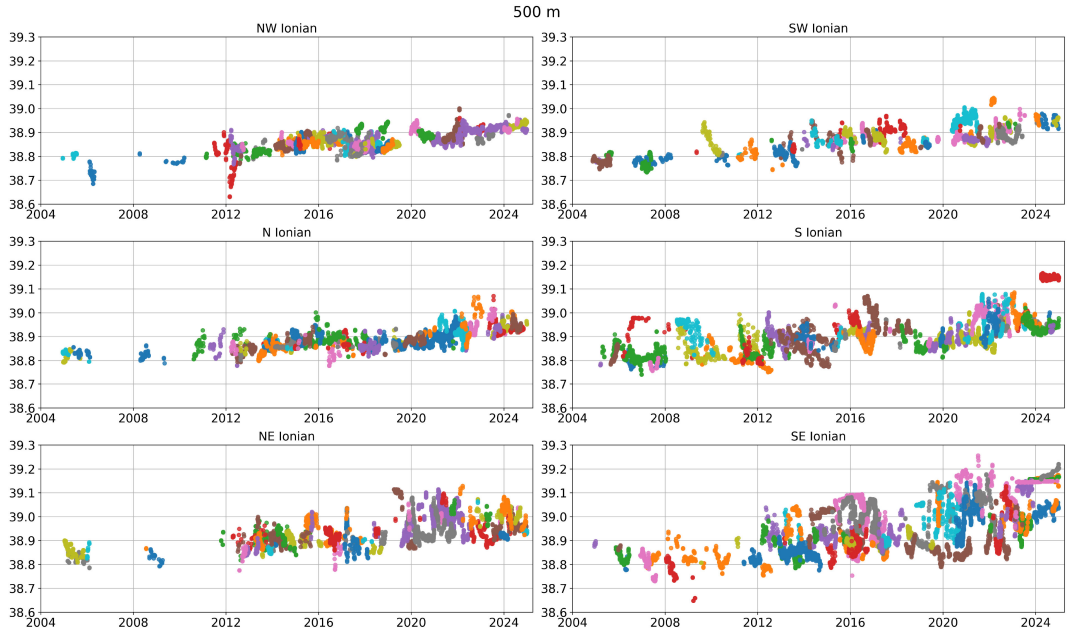

FIGURE 5
Time series for *S* at 500 m depth, each subplot for one of the 6 Ionian sub-basins. Each color represents a different float.

reaches a highest rate of 0.27 /decade at 100 m in the SE Ionian, followed by 0.18 /decade in the SE and NE Ionian, generally decreasing with depth and overall positive except at 100 m in the S and SW Ionian (Figure 7b). PDA has a third of statistically insignificant trends (p-value>0.01), with increasing PDA of up to 0.12 kgm^{-3} /decade at 100 m for the SE and the NE Ionian (Figure 7c). NW Ionian also shows an increase in salinity at the surface, diminishing with depth, whereas the SW shows a decreasing trend in density at all depths where trends are significant.

Although interannual positive trends in temperature and salinity are visible across most regions, the abrupt intensification during 2022–2024 emerges most clearly at intermediate and deep layers, particularly below 1000 m in the S and SE Ionian (see

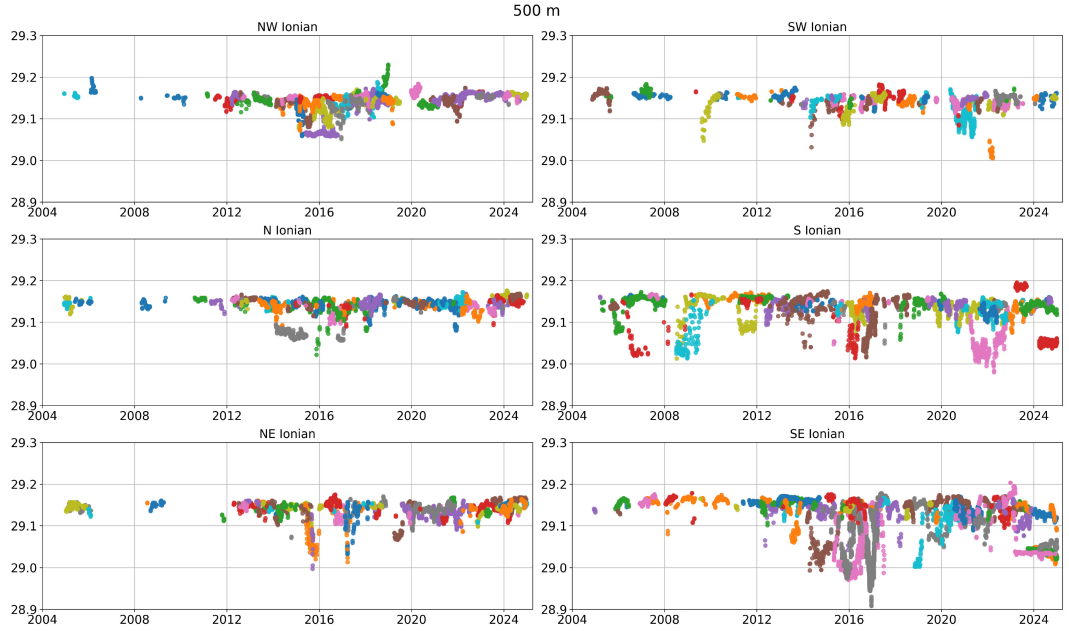

FIGURE 6
Time series of *PDA* at 500 m depth, each subplot for one of the 6 Ionian sub-basins. Each color represents a different float.

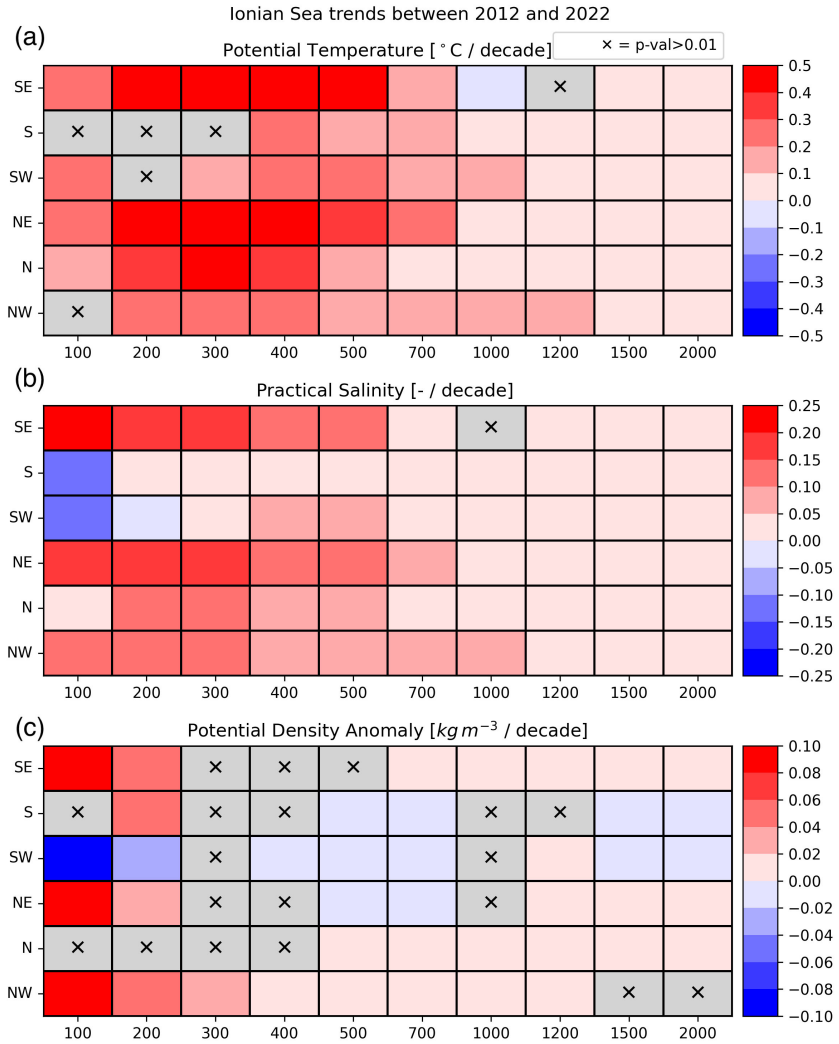

FIGURE 7
Linear trends between 2012 and 2022 for: **(a)** *T*, **(b)** *S* and **(c)** *PDA*, for different depths (x-axis) and regions (y-axis). Grey crossed boxes are statistically insignificant (p>0.01).

Supplementary Figures S7-S9). The magnitude and vertical coherence of these anomalies exceed the variability observed during earlier warm episodes (e.g. 2015–2017), suggesting that the recent changes are not simply part of the quasi-decadal modulation previously recorded in the basin. For this reason, the period 2023–2024 was excluded from the linear trend estimates—to avoid biasing decadal rates—but is analyzed separately as a distinct event through the 2024–2022 differences shown in Figure 8. Localized processes such as downwelling associated with the Mid-Ionian Jet meanders or enhanced convection within the Pelops Gyre could have contributed to the downward propagation of heat and salt; however, comparable signals were not documented with such intensity in the earlier record. These observations therefore motivated the subsequent analysis of atmospheric forcing anomalies (Section 3.3), aimed at identifying large-scale drivers capable of producing the 2022–2024 deep thermohaline shift.

Focusing on recent changes, the annual median differences between 2024 and 2022 were obtained per region at selected depths (Figure 8). Major discrepancies are observed in the SE Ionian, where temperature difference ranges from 0.72°C at 100 m to up to 1.81°C at 1000 m depth, and similar to the S Ionian, where the differences vary from around 1°C between 300 and 500 m and up to 1.5°C at 700 m (Figure 8a). Salinity also shows largest differences in S and SE Ionian at intermediate depths (Figure 8b): from 0.26 at 700 m to up to 0.4 at 1000 m for SE and 0.21 and 0.34 at 500 and 700 m at the S Ionian. SW Ionian has the largest salinity difference at 100 m, i.e., 0.31. PDA consequently decreases in SE and S Ionian at all depths examined except at 100 m for S Ionian, up to -0.14, -0.15 kgm^{-3} at 100–200 m in SE Ionian (Figure 8c). In contrast, a drastic increase is seen in SW Ionian due to a significant salinification at 100 and 200 m, (0.25 and 0.20 kgm^{-3}, respectively). In the northern Ionian basins, *PDA* decrease at 100 m ranges between -0.11 and -0.13 kgm^{-3}.

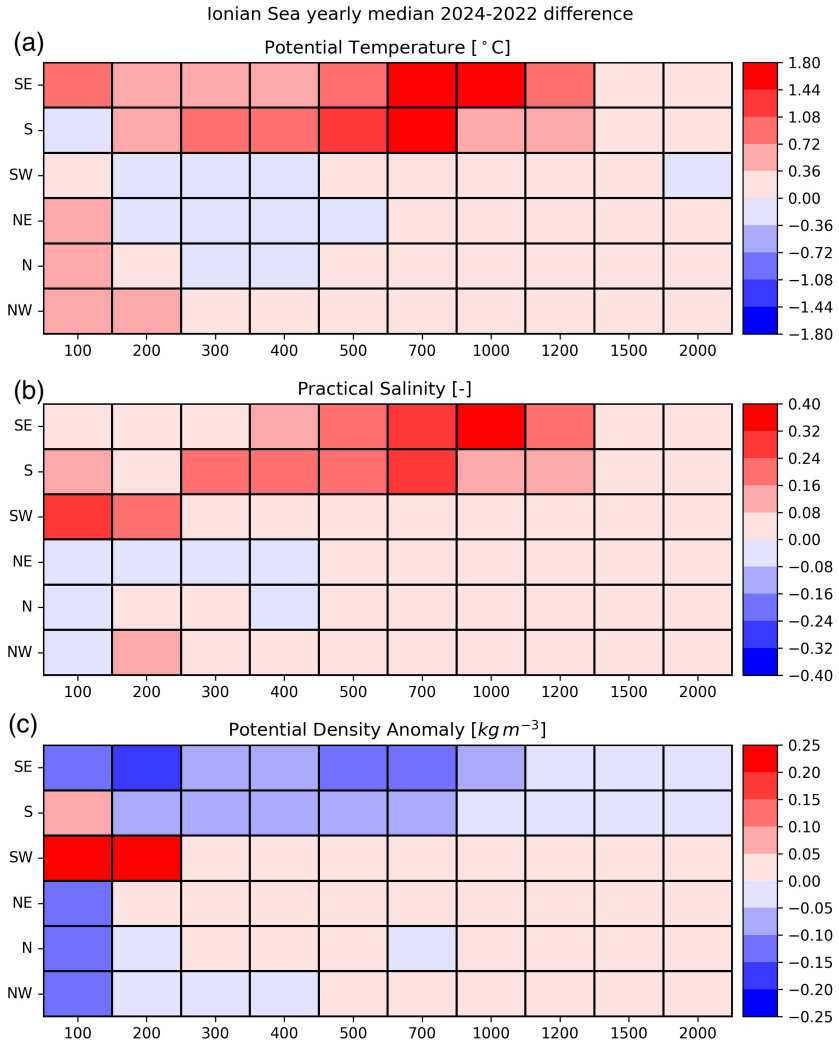

FIGURE 8
Annual median difference between 2024 and 2022 for: **(a)** *T*, **(b)** *S* and **(c)** *PDA*, for different depths (x-axis) and regions (y-axis).

3.3 Air-sea heat, water and momentum exchanges

To understand the drivers of trends and abrupt changes in thermohaline properties in over the past decade, we examined summer (June-August) and winter (December-March) anomalies of total heat flux, wind stress and evaporation-precipitation difference (E-P), for the period 2012–2024 relative to the 1980–2010 baseline. Summer anomalies reveal predominantly negative total heat fluxes from 2013 to 2019 and again in 2021, 2022 and 2024, with lowest values in the Levantine basin (up to -9 Wm^{-2} in 2014, Figure 9a). In contrast, 2019 and 2020 exhibit a sharp shift towards positive heat fluxes (12 Wm^{-2} in the Ionian Sea in 2019 and close to 10 Wm^{-2} in the Levantine basin the year after). Another increase is seen in 2023, when the Levantine basin reached highest values (7 Wm^{-2}). On average, however, summer total heat fluxes for the 2012–2024 remain negative, which might indicate, through reduced latent heat fluxes, a weakening of the Etesian winds. This interpretation is supported by looking at wind stress summer anomalies, which are predominantly negative over the past 12 years, with the exception in 2013 and 2014 across all 3 regions, and in 2016, 2018, 2020 and 2023 in the Ionian Sea (Figure 9b). Summer E-P anomalies are almost always positive except in 2015 (Levantine basin and Aegean Sea), 2017 (Ionian Sea), and 2023 (all three regions, with the anomaly reaching up to -0.3 mm/day, Figure 9c). On average, E-P anomalies reveal much drier and warmer conditions compared to the 1980–2010 climatology, with the largest deviations in 2012 in the Ionian Sea (above 0.4 mm/day), followed by 2013, 2014, 2016, 2021 and 2024 in the Levantine basin (around 0.3 mm/day), whilst the Aegean Sea generally shows smallest differences, reaching up to 0.13 mm/day in 2021 (Figure 9c).

Winter anomalies reveal mostly negative heat fluxes, except in 2014, 2016, 2018 and 2020 in the Ionian Sea, and in 2023 and 2024 across the three regions considered (Figure 10a). The strongest negative flux anomalies are seen in the winter 2021/2022 (-40 Wm^{-2} in the Levantine basin and -30 Wm^{-2} in the Ionian Sea), indicating enhanced vertical mixing, consistent with positive wind stress

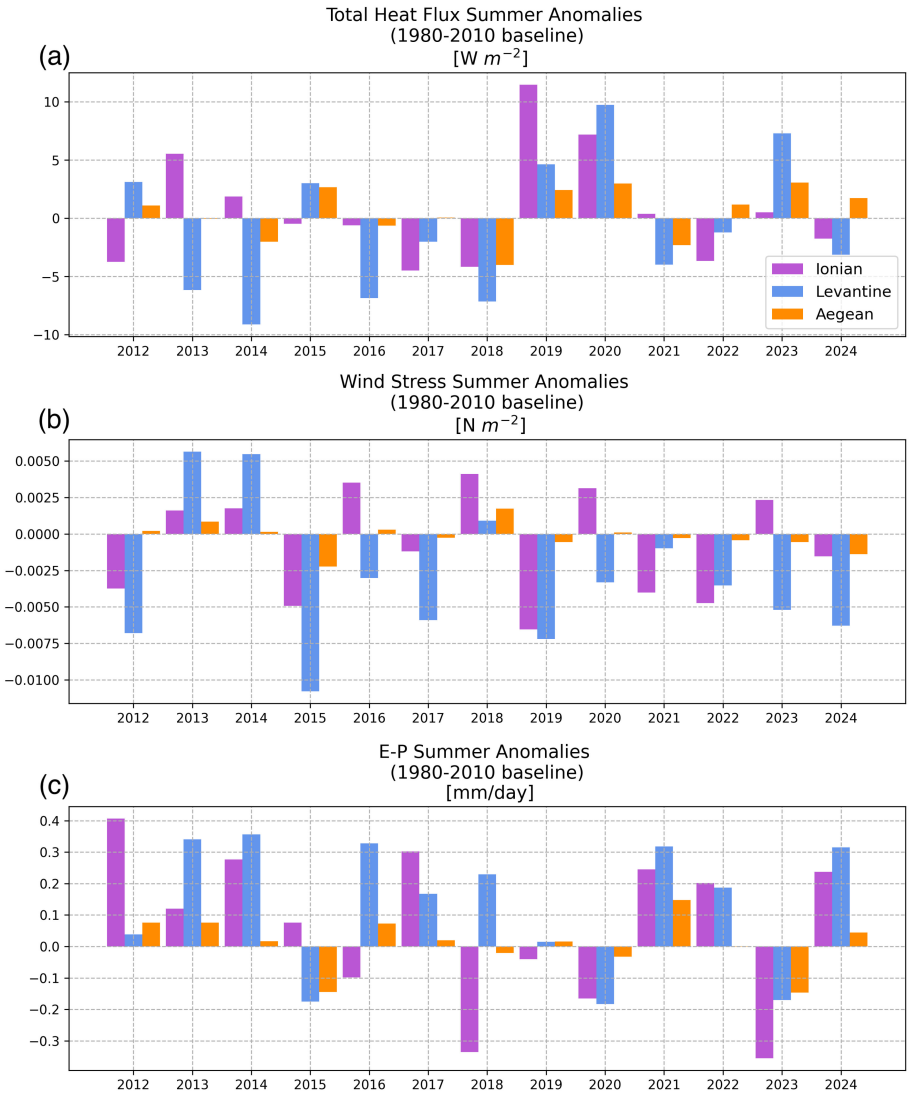

FIGURE 9
ERA5 summer anomalies of: **(a)** total heat flux, **(b)** wind stress and **(c)** evaporation-precipitation (E-P) rates.

anomalies during the same winter (Figure 10b). Wind stress anomalies turn negative in the last two years (up to -0.02 Nm^{-2}), coinciding with positive anomalies in both heat flux and E-P (Figure 10c). E-P anomalies are predominantly positive throughout the entire period, with exceptions in 2014 and 2019 (Figure 10c).

Overall, the ERA5 reanalysis reveals that the winter of 2021/2022 was characterized by exceptionally strong surface-forcing anomalies across the Eastern Mediterranean. In the Ionian Sea, total heat-flux anomalies reached about -30 Wm^{-2}, indicating an anomalous upward (ocean-to-atmosphere) heat loss conducive to deep convective mixing. Simultaneously, wind-stress anomalies were positive, with values up to 0.02 Nm^{-2} above the climatological mean, favoring enhanced surface stress and vertical momentum transfer. The evaporation–precipitation (E–P) balance also showed a sustained positive anomaly (ca. 0.3 $mmday^{-1}$), signifying intensified net evaporation and surface salinification. The co-occurrence of these flux, stress, and water loss anomalies suggests that winter 2021/2022 provided favorable conditions for deep ventilation and the downward propagation of warm, saline surface waters into intermediate layers. This interpretation supports the hypothesis that the 2022–2024 thermohaline shift identified in Figure 8 originated, at least in part, from anomalous surface-forcing conditions during that winter.

4 Discussion

Our results demonstrate that the Ionian Sea experienced an abrupt thermohaline shift between 2022 and 2024, superimposed on a decade-long period (2012–2022) of progressive warming and salinification documented by the Argo record. Earlier observations prior to 2012, although sparser, are consistent with this long-term tendency but are not sufficient to quantify trends with comparable

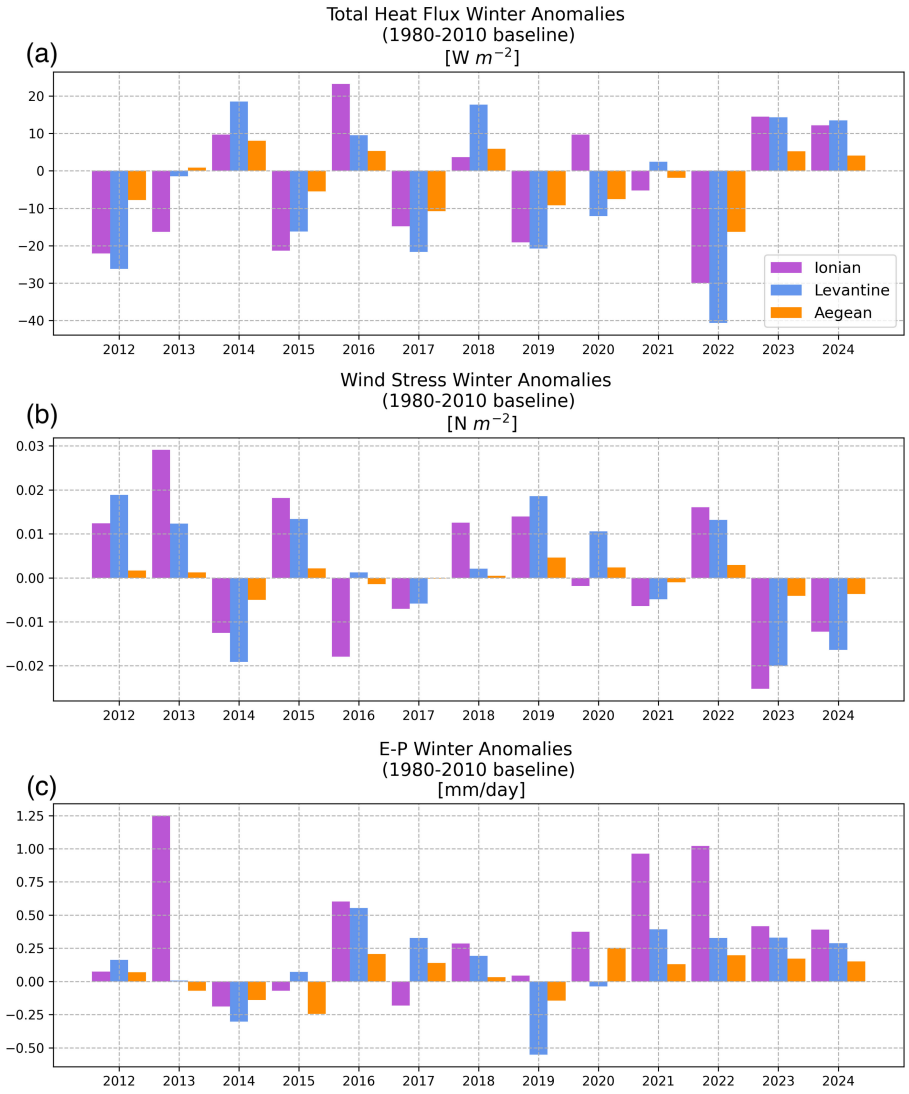

FIGURE 10
ERA5 winter anomalies of: **(a)** total heat flux, **(b)** wind stress and **(c)** evaporation-precipitation (E-P) rates.

statistical robustness. Largest anomalies occurred in the southern and south-eastern Ionian at 300–1200 m, where temperature rose by 0.7–1.8°C and salinity increased by 0.24–0.40, peaking near 700–1000 m over 2022–2024. The persistent positive trends in temperature and salinity observed over many decades are likely to alter the climatology of the Ionian and Mediterranean seas and consequently affect thermohaline circulation, which is projected to weaken and shoal under future climate conditions.

To quantify these changes, we compared the Argo-based climatology with the historical climatology provided by (Manca et al., 2004). The latter was derived from bottle samples collected mainly between the 1950s and the end of the 20th century at standard oceanographic depths, supplemented by CTD and XBT profiles during the last two decades of that century. Figure 11 shows seasonal temperature climatologies for the upper 2000 m of the southern Ionian Sea (region DJ5 in Figure 6 of Manca et al. (2004), corresponding to the southern sections of our sub-basins SW, S, and SE), based on both Manca et al. (2004) and Argo data from 2001–2024, with the Argo climatology adapted to standard depths. It is important to note that the Manca et al. (2004) climatology largely represents pre-EMT conditions, whereas our Argo-based climatology reflects the post-EMT period. Consequently, part of the deep-layer differences between the two datasets likely arises from Aegean-sourced intrusions that occurred during and after the EMT, rather than from recent decadal trends alone.

The comparison reveals that temperatures in the upper layers increased by more than 2°C during spring and summer, with additional warming of about 0.15°C at intermediate and deep layers. Below 500 m, salinity increased by 0.2–0.4, with the highest anomalies in summer, while the maximum salinity increase (up to 0.3) was found between 50 and 200 m — coinciding with the typical upper core of the Levantine Intermediate Water (LIW). These patterns also suggest a shoaling of the LIW between the two climatologies. Taken together, these

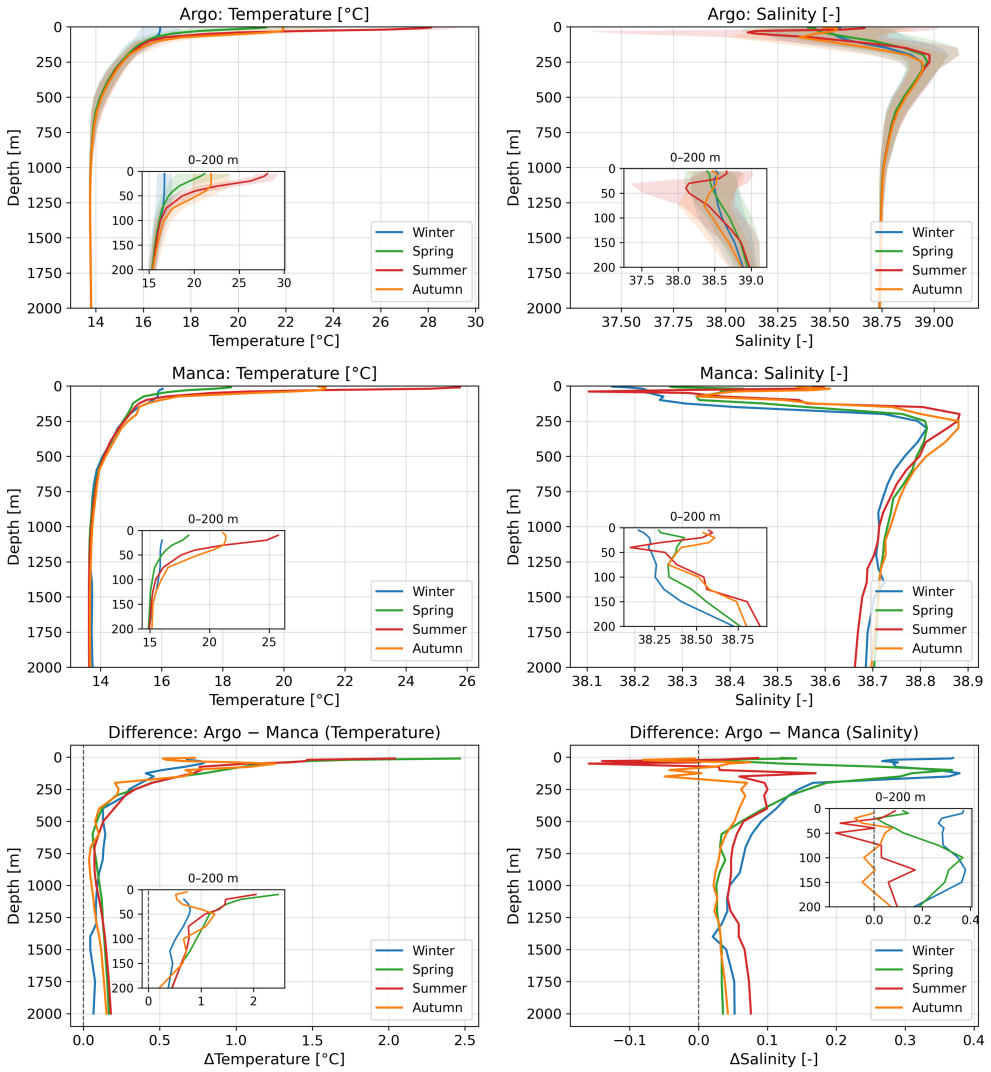

FIGURE 11
Seasonal climatological values for T and S from Argo data (first row), historical data from Manca et al. (2004) (second row) and their difference (third row). Shaded parts denote mean and standard deviation values from Argo data.

abrupt multi-decadal changes — substantially exceeding global averages — underscore the Mediterranean's role as a climate change hot spot (Giorgi, 2006).

In the following, we address uncertainties related to Argo measurements, place these anomalies in the context of observed changes in the Eastern Mediterranean and Adriatic, discuss implications for the BiOS mechanism, review possible future evolution under climate projections, and consider biogeochemical consequences.

4.1 Uncertainties in Argo measurements and sampling heterogeneity

Argo floats are freely drifting platforms and therefore sample the basin heterogeneously in both space and time (Figure 1, top). Such irregular coverage can introduce biases when data are spatially aggregated (Hadfield et al., 2007; Good et al., 2013). Nevertheless, our results are supported by a large number of profiles from multiple floats (Figure 1, bottom) evenly distributed between six Ionian sub-basins, as also shown by Figures 4-6 and the float-resolved time series in the Supplement, where data are color-coded by float ID. Certainly, the uncertainty in temperature and salinity trends might reach substantial levels in the upper ocean shallower than the seasonal thermocline, e.g., at 100 m in our estimates in the Ionian Sea. However, the water masses in the Mediterranean exhibit much lower horizontal variability in deeper layers due to their approximate residence time of 100 years (Roether et al., 1996), therefore the trends and abrupt shifts of our analysis are much stronger than differences in temperature and salinity resulting from space-time inhomogeneity. Nevertheless, horizontal variability in the deeper layers cannot be entirely neglected, as differences in dense-water formation sources (Adriatic versus Aegean) and their episodic intrusions can imprint regional contrasts in deep-water

properties, even within the generally long residence times of Eastern Mediterranean Deep Water (e.g., Cardin et al., 2015). A further source of uncertainty arises from the use of real-time data and drifts in salinity sensors. Accuracy is typically ~0.01 °C in real time and ~0.002 °C in delayed mode for temperature, and 0.02–0.05 in real time and 0.01–0.02 in delayed mode for salinity. Further, salinity drifts were expected to be higher in the earlier phase of the Argo program (Wong et al., 2023; Liu et al., 2024), thus the early observations would exhibit a larger positive salinity bias than the recent measurements. Hence, such bias can even lower real trend estimates. While such errors may affect short-term variability or small-scale gradients, the magnitude of the observed 2022–2024 changes is unequivocal and several orders of magnitude larger than measurement uncertainties. We therefore consider the reported anomalies robust.

4.2 Observed changes in the Eastern Mediterranean Sea

The Mediterranean, particularly its eastern basin, is undergoing rapid warming and salinification, with accelerated trends in both surface and subsurface waters (Skliris et al., 2024). At its source in the Levantine basin and between 1978 and 2014, LIW and LSW were warming at ~0.3°C and 1.2°C per decade and salinifying at ~0.05 and 0.03 per decade (Ozer et al., 2017), with anomalies accumulating downstream, i.e., in the Western Mediterranean, during periods of weak convection (Margirier et al., 2020). Conjointly, the deep southern Adriatic has also seen unprecedented warming (0.8°C) and salinification (0.2) over the past decade (2012-2024), altering dense-water formation properties, partially due to increased LIW-driven salt inflow, but mostly due to local freshwater and thermal forcing (Kubin et al., 2023; Terzić et al., 2025a). Warmer, saltier deep Ionian waters may therefore increase vertical stratification in the dense-water source regions - as already found in the Western Mediterranean (Margirier et al., 2020) - and reduce the density-driven ventilation due to enhanced buoyancy forcing necessary for deep overturning, potentially slowing deep-water renewal across the Eastern Mediterranean.

Abrupt jumps in 2023/2024, especially in the northwestern Ionian at 1000 and 1500 m (Supplement), may be linked to changes already observed in the southern Adriatic where dense water has warmed and salinified at unprecedented rates (Terzić et al., 2025a). The inflow of saltier LIW into the Adriatic has progressively modified the properties of locally formed dense waters, particularly since 2022. Because Adriatic Dense Water originates both from wintertime shelf mixing in the northern Adriatic and from open-ocean convection within the Southern Adriatic Pit, enhanced salinity of the source waters can increase the density and temperature of the resulting deep outflows (Bensi et al., 2013; Martellucci et al., 2025). These modified dense waters subsequently exit the basin through the Strait of Otranto, influencing the temperature and salinity characteristics of the deep Ionian Sea (Sellschopp and Álvarez, 2003). In contrast, temperature and salinity jumps in the southeastern Ionian appear consistent with changes in winter surface forcing during 2021/2022. Enhanced heat losses and stronger wind-stress forcing during that winter likely increased vertical mixing and facilitated penetration of LSW and LIW to greater depths, most clearly seen from T and S jumps in the SE Ionian. In the subsequent two years, following the timscales to which saline waters travel between different Eastern Mediterraean basins (Bensi et al., 2016; Taillandier et al., 2022), negative wind-stress anomalies, combined with positive heat flux and excess evaporation over precipitation, may have reduced convective capability, keeping the deepened warm and saline waters in intermediate and deep layers, gradually propagating within the basin and towards the Western Mediterranean. Consequently, a continued warming and salinification of intermediate waters can be expected in the main dense-water formation regions, with the associated anomalies propagating on different timescales - from about one to several years in the Adriatic Sea (Mihanović et al., 2015) to nearly a decade in the Western Mediterranean and Gulf of Lions (Roether et al., 1998; Vecchioni et al., 2023). The 2021/2022 winter conditions were reported to have played also a role in the high salinity driven dense water formation in the Aegean Sea, which was, due to its intense warming, spatially limited and prevented the dense water to spread outside the region (Potiris et al., 2024a).

4.3 BiOS in the context of evolving Adriatic and Eastern Mediterranean conditions

Although our observations are limited to the upper 2000 m and do not directly resolve the deepest layers where Adriatic and Aegean dense waters accumulate, the recorded changes at intermediate depths are highly relevant to the BiOS dynamics. The BiOS is fundamentally governed by density and salinity gradients between the eastern and western Ionian, which control the vorticity balance and, consequently, the polarity of the gyre circulation. The pronounced 2022–2024 warming and salinification in the 300–1200 m layer, especially in the southern and south-eastern Ionian (Figures 7, 8), likely enhanced these density contrasts, preconditioning the basin for future changes in the BiOS regimes. Such intermediate-layer anomalies can modify the advection of Levantine and Adriatic-origin waters, thereby influencing both the timing and intensity of BiOS reversals. Hence, variability at intermediate depths—rather than only deep Adriatic processes—may exert a more immediate influence on the evolving BiOS regime than previously assumed.

The relationship between the observed thermohaline anomalies and BiOS can be inferred from the regional patterns presented in Section 3.2, where the strongest warming and salinification were confined to the southern and south-eastern Ionian. These regions correspond to the zones most sensitive to BiOS-driven exchanges between Atlantic- and Levantine-origin waters, suggesting that the 2022–2024 shift may represent a reorganization of this circulation regime rather than an isolated local event. With the abrupt warming and salinification now observed in the Ionian, a key question is whether BiOS itself will be affected. BiOS hinges on salinity and

density contrasts, alternating between Atlantic-origin and Eastern Mediterranean waters through cyclonic and anticyclonic regimes (Gačić et al., 2010; Civitarese et al., 2023). These contrasts changed considerably in the past (Sampatakaki et al., 2021), while altimeter observations of the BiOS phases and strength indicate a weakening in recent years (Meli, 2024). BiOS reversals have become milder in the 2010s–2020s compared with the 1990s–2000s, a period marked by stronger dense water formation that intensified the BiOS phases (Klein et al., 1999; Mihanović et al., 2015). This weakening is consistent with a documented decline in winter heat loss at Mediterranean dense water formation sites (Josey and Schroeder, 2023). If the deep Ionian becomes uniformly warmer and saltier due to rapid warming and salinization in the Adriatic dense waters, the contrasts that sustain BiOS could diminish. This may dampen, alter, or even lock BiOS phases instead of preserving its quasi-decadal oscillation (Eusebi Borzelli and Carniel, 2023). On the other hand, laboratory and numerical experiments indicate that episodic strong dense-water formation can trigger abrupt BiOS polarity switches; thus, even under warming, extreme convection could still produce sudden regime shifts (Rubino et al., 2020). Given the Mediterranean's role as a saline source to the global thermohaline circulation through the Gibraltar outflow (Aldama-Campino and Döös, 2020; Saporta-Katz et al., 2024), the evolution of BiOS has implications that extend to the Atlantic circulation systems.

4.4 Future evolution under projected changes

Multi-model and regional projections consistently indicate continued increases in surface and intermediate temperatures and salinities (Soto-Navarro et al., 2020; Parras-Berrocal et al., 2024). Ionian water masses are expected to further warm and salinify, altering LIW and intermediate layers that feed the Sicilian Channel, thereby changing the properties of waters exported westward and impacting Western Mediterranean circulation and thermohaline balance (Parras-Berrocal et al., 2024). Regional climate models also project reduced net heat loss (Soto-Navarro et al., 2020), driven by increased shortwave, net longwave, and sensible heat fluxes associated with greenhouse forcing and reduced cloud cover (Dubois et al., 2012).

High-resolution projections for the Adriatic suggest that future warming may increase local buoyancy loss via higher evaporation, even as bora winds weaken. Dense-water formation may thus persist, but with modified volumes, transport routes, and connectivity, thereby altering Adriatic preconditioning of the Ionian and the forcing of BiOS (Denamiel et al., 2021, Denamiel et al., 2025). If the Ionian and Levantine basins become uniformly warmer and saltier, the density contrasts that sustain BiOS could weaken further, dampening oscillations or locking the system in one phase depending on the sign of the net forcing. Reviews and mechanism studies emphasize that BiOS depends on the balance of buoyancy inputs from dense-water formation and wind/boundary forcing (Eusebi Borzelli and Carniel, 2023; Civitarese et al., 2023). According to Parras-Berrocal et al. (2024), projected warming will not increase the frequency of the anticyclonic phase in the northern Ionian, which is expected to remain predominantly cyclonic, with reversals only 15–20% of the time during the simulated periods. Recent analyses (Ocean State Report 6, de Boisséson et al., 2022) further indicate a progressive weakening of the anticyclonic mode's amplitude relative to the cyclonic one. Importantly, possible transitions between the two circulation states depend strongly on the volume and density of the dense waters entering the Ionian from the Adriatic or Aegean Seas, as previously demonstrated during the Eastern Mediterranean Transient (Civitarese et al., 2023).

The magnitude of the 2022–2024 anomalies documented in this study provides an empirical analogue for the changes projected by regional climate models, which consistently indicate continued warming and salinification of intermediate layers (Section 3.2). These recent observations therefore offer a near-term example of the processes expected to intensify under future forcing.

4.5 Biogeochemical implications

Elevated temperature and altered stratification are linked to declining biomass across the Ionian and other regions of the Eastern Mediterranean (Reale et al., 2022). Projected warming, salinification, and changes in dense-water formation may further reduce ventilation and oxygenation of deep layers, raising the risk of hypoxia and large-scale biogeochemical reorganization, such as already observed in the south-eastern Mediterranean (Sisma-Ventura et al., 2021). Nutrient dynamics are also likely to be affected: reduced vertical mixing might suppress nutrient recycling to surface layers, undermining productivity (Kotta and Kitsiou, 2019; Salgado-Hernanz et al., 2019) and disrupting food webs. On the other hand, recent warming and salinification of LIW have reduced its density and shoaled its core into the lower photic zone, enhancing nutrient supply and supporting a long-term rise in chlorophyll-a and productivity (Ozer et al., 2022).

Evidence from the 2017 high-salinity Adriatic event points to reduced bacterial production and shifts in microbial community composition, providing a potential analog for future conditions (Beg Paklar et al., 2020).

The BiOS regimes are known to affect biogeochemistry within the Mediterranean basins (Civitarese et al., 2023), primarily in the Ionian Sea through large-scale displacements of the nutricline (Civitarese et al., 2010; Lavigne et al., 2018). However, similar effects have also been quantified in basins both near and far from the Ionian. For example, elevated nutrient levels appear with a lag of a few years in neighboring regions such as the Adriatic and the Sicily Channel (Mihanović et al., 2015; Placenti et al., 2022; Patti et al., 2025), while BiOS-related nutrient oscillations extend as far as the eastern Levantine Basin (Ozer et al., 2017). Consequently, changes in the BiOS—beyond those described in the previous paragraph—may reshape the available nutrient pool under future climate conditions and substantially influence the decadal variability of biogeochemistry, productivity, and related processes, including the migration of invasive species (Glamuzina et al., 2024).

The abrupt 2022–2024 warming and salinification of intermediate waters (Figures 7, 8) imply stronger vertical stratification, reduced deep ventilation, and altered nutrient fluxes — conditions that directly affect oxygen and productivity patterns across the Ionian and adjacent basins.

The magnitude and coherence of the 2022–2024 changes suggest that biogeochemical fields shifted alongside physical ones, consistent with recent findings in the Adriatic and surface Ionian (Terzić et al., 2025a, Terzić et al., 2025b). Sustained multidisciplinary monitoring—including Argo, biogeochemical Argo (BGC-Argo), gliders, and moorings—will be essential to track these changes, identify drivers, and evaluate whether the current anomalies represent a transient event or the onset of a new long-term regime.

5 Conclusions

Using 23 years (2001–2024) of Argo float profiles, we documented significant thermohaline variability across the Ionian Sea. Between 2022 and 2024, intermediate waters (300–1200 m) in the southern and south eastern Ionian warmed by 0.7–1.8 °C and salinity increased by 0.24–0.40, with maxima near 700–1000 m. These anomalies were most pronounced in the S and SE Ionian, where vertical and horizontal gradients intensified.

ERA5 reanalysis indicates that anomalous surface forcing in winter 2021/2022 played a central role. Strong negative heat-flux anomalies, intensified wind stress, and enhanced evaporation relative to precipitation favored deep convective mixing, transporting warm, saline surface waters to depth. The reduced renewal from the Adriatic and the enhanced presence of Levantine waters provided an additional source of salinity, shaping the spatial structure of the observed anomalies.

Such changes could alter the balance between Adriatic- and Aegean-sourced deep waters that together sustain the Eastern Mediterranean Deep Water (EMDW). A persistently warmer and more saline Ionian would likely reduce the density contrast between surface and intermediate layers in the southern Adriatic, thereby weakening local dense-water formation and diminishing the Adriatic contribution to the deep thermohaline cell. At the same time, enhanced salinity in the southern and southeastern Ionian could favor increased influence of Aegean-origin dense waters, particularly under conditions similar to those observed during the Eastern Mediterranean Transient. This redistribution would modify the renewal pathways and physical characteristics of the EMDW, with potential consequences for ventilation, oxygen content, and long-term heat and salt storage across the basin.

Beyond circulation, the physical anomalies are likely to drive biogeochemical adjustments. Stronger stratification and warmer subsurface layers reduce vertical nutrient supply, while episodic convection events ventilate intermediate and deep layers. The magnitude and coherence of the 2022–2024 changes suggest that nutrient cycling, oxygen distributions, and ecosystem dynamics have shifted alongside the physical fields, with potential impacts on plankton and higher trophic levels.

Our findings underscore the Ionian Sea as a hotspot of Mediterranean climate variability. The 2022–2024 anomalies highlight how short-lived but intense surface forcing can trigger basin-scale adjustments, potentially marking the onset of a new regime. Sustained multidisciplinary monitoring—through Argo (including BGC-Argo), gliders, moorings, and models—will be essential to determine whether the Ionian remains in this warmer, saltier state, to attribute its drivers, and to assess its long-term consequences for Mediterranean and Atlantic circulation.

Data availability statement

All data used in this study are openly available. Argo float profiles were accessed through the Python library argopy (https://pypi.org/project/argopy/). ERA5 reanalysis data are provided by the Copernicus Climate Change Service (C3S) and can be freely downloaded from the Copernicus Climate Data Store (https://cds.climate.copernicus.eu/). Historical temperature and salinity profiles for the Southern Ionian Sea were obtained from the MEDAR/MEDATLAS II collections hosted by Ocean Data View (AWI). We used the CTD and merged T&S ("allTS") packages available at https://odv.awi.de/data/ocean/medatlasii/ (accessed 12 September 2025). For reproducibility, direct downloads are provided on that page (e.g., MedatlasII_Ctd.zip and MedatlasII_allTS.zip). We used only temperature and salinity variables from these collections. We accessed and exported the data using Ocean Data View (ODV, Schlitzer, 2018).

Author contributions

ET: Conceptualization, Formal analysis, Investigation, Methodology, Validation, Visualization, Writing – original draft, Writing – review & editing. IV: Conceptualization, Formal analysis, Funding acquisition, Investigation, Methodology, Project administration, Supervision, Writing – original draft, Resources, Validation, Writing – review & editing.

Funding

The author(s) declared financial support was received for this work and/or its publication. The research has been carried out with the support of the Croatian Science Foundation through research projects GLOMETS (Grant IP-2022-10-3064), C3PO (Grant IP2022-9139), project AdriaClimPlus (Grant ITHR0200333) and the incoming mobility scheme for postdoctoral researchers (MOBDOL-2023-12, ET).

Acknowledgments

We gratefully acknowledge the European Argo program and its data providers and developers for their invaluable efforts in producing and maintaining the datasets used in this study. We also thank ECMWF and the Copernicus Climate Change Service (C3S) for developing and maintaining the ERA5 reanalysis and for ensuring open access to these data (https://cds.climate.copernicus.eu/). In addition, we are grateful to the developers of the MapPlotter (https://pypi.org/project/MapPlotter/2.2.0/, last access: 15 September 2025) and Basins (https://pypi.org/project/Basins/, last access: 15 September 2025) libraries for providing effective and visually appealing tools for data visualization and spatial analysis. Finally, we thank the argopy (https://pypi.org/project/argopy/, last access: 15 September 2025) development team for making Argo data analysis more accessible and user-friendly.

Conflict of interest

The authors declared that this work was conducted in the absence of any commercial or financial relationships that could be construed as a potential conflict of interest.

The handling editor JC declared a past co-authorship with the author ET.

Generative AI statement

The author(s) declared that generative AI was not used in the creation of this manuscript.

Any alternative text (alt text) provided alongside figures in this article has been generated by Frontiers with the support of artificial intelligence and reasonable efforts have been made to ensure accuracy, including review by the authors wherever possible. If you identify any issues, please contact us.

Publisher's note

Supplementary material

The Supplementary Material for this article can be found online at: https://www.frontiersin.org/articles/10.3389/fmars.2025.1718186/full#supplementary-material

References

Aldama-Campino, A., and Döös, K. (2020). Mediterranean overflow water in the north atlantic and its multidecadal variability. *Tellus A: Dyn. Meteorol. Oceanogr.* 71, 1—10. doi: 10.1080/16000870.2018.1565027

Androulidakis, Y., Kolovoyiannis, V., Makris, C., and Krestenitis, Y. (2024). Evidence of 2024 summer as the warmest during the last four decades in the Aegean, Ionian, and Cretan seas. *J. Mar. Sci. Eng.* 12, 2020. doi: 10.3390/jmse12112020

Artale, V., Falcini, F., Marullo, S., Bensi, M., Kokoszka, F., Iudicone, D., et al. (2018). Linking mixing processes and climate variability to the heat content distribution of the Eastern Mediterranean abyss. *Sci. Rep.* 8, 11317. doi: 10.1038/s41598-018-29343-4

Batistić, M., Garić, R., and Molinero, J. (2014). Interannual variations in Adriatic Sea zooplankton mirror shifts in circulation regimes in the Ionian Sea. *Clim. Res.* 61, 231—240. doi: 10.3354/cr01248

Beg Paklar, G., Vilibić, I., Grbec, B., Matić, F., Mihanović, H., Džoić, T., et al. (2020). Record-breaking salinities in the middle Adriatic during summer 2017 and concurrent changes in the microbial food web. *Prog. Oceanogr.* 185, 102345. doi: 10.1016/j.pocean.2020.102345

Bensi, M., Rubino, A., Cardin, V., Hainbucher, D., and Mancero-Mosquera, I. (2013). Structure and variability of the abyssal water masses in the Ionian Sea in the period 2003-2010. *J. Geophys. Res. Oceans* 118, 931–943. doi: 10.1029/2012JC008178

Bensi, M., Velaoras, D., Meccia, L. V., and Cardin, V. (2016). Effects of the Eastern Mediterranean Sea circulation on the thermohaline properties as recorded by fixed deep-ocean observatories. *Deep-Sea Res. Part I: Oceanogr. Res. Papers* 112, 1–13. doi: 10.1016/j.dsr.2016.02.015

Berline, L., Doglioli, A. M., Petrenko, A., Barrillon, S., Espinasse, B., Le Moigne, F. A. C., et al. (2021). Long-distance particle transport to the central Ionian Sea. *Biogeosciences* 18, 6377—6392. doi: 10.5194/bg-18-6377-2021

Borile, F., Pinardi, N., Lyubartsev, V., Ghani, M. H., Navarra, A., Alessandri, J., et al. (2025). The Eastern Mediterranean Sea mean sea level decadal slowdown: the effects of the water budget. *Front. Clim.* 7. doi: 10.3389/fclim.2025.1472731

Budillon, G., Bue, N. L., Siena, G., and Spezie, G. (2010). Hydrographic characteristics of water masses and circulation in the Northern Ionian Sea. *Deep Sea Res. Part II: Topical Stud. Oceanogr.* 57, 441—457. doi: 10.1016/j.dsr2.2009.08.017

Cardin, V., Civitarese, G., Hainbucher, D., Bensi, M., and Rubino, A. (2015). Thermohaline properties in the Eastern Mediterranean in the last three decades: is the basin returning to the pre-EMT situation? *Ocean Sci.* 11, 53–66. doi: 10.5194/os-11-53-2015

Chen, G., and Wang, X. (2016). Vertical structure of upper-ocean seasonality: Annual and semiannual cycles with oceanographic implications. *J. Clim.* 29, 37–59. doi: 10.1175/JCLI-D-14-00855.1

Civitarese, G., Gačić, M., Batistić, M., Bensi, M., Cardin, V., Dulčić, J., et al. (2023). The BiOS mechanism: History, theory, implications. *Prog. Oceanogr.* 216, 103056. doi: 10.1016/j.pocean.2023.103056

Civitarese, G., Gačić, M., Lipizer, M., and Borzelli, G. L. E. (2010). On the impact of the Bimodal Oscillating System (BiOS) on the biogeochemistry and biology of the Adriatic and Ionian seas (Eastern Mediterranean). *Biogeosciences.* 7, 3987–3997. doi: 10.5194/bg-7-3987-2010

de Boisséson, E., Balmaseda, M., Mayer, M., and Zuo, H. (eds.) (2022). Copernicus Ocean State Report – Issue 6. *Supplement to the J. Oper. Oceanogr.*. 15 (Supplement 1), s1–s220. doi: 10.1080/1755876X.2022.2095169

Denamiel, C., Pranić, P., Ivanković, D., Tojčić, I., and Vilibić, I. (2021). Performance of the Adriatic Sea and Coast (AdriSC) climate component – a COAWST V3.3-based coupled atmosphere–ocean modelling suite: atmospheric dataset. *Geosci. Model. Dev.* 14, 3995—4017. doi: 10.5194/gmd-14-3995-2021

Denamiel, C., Tojčić, I., and Pranić, P. (2025). A new vision of the Adriatic dense water future under extreme warming. *Ocean Sci.* 21, 37—62. doi: 10.5194/os-21-37-2025

Dubois, C., Somot, S., Calmanti, S., Carillo, A., Déqué, M., Dell'Aquilla, A., et al. (2012). Future projections of the surface heat and water budgets of the Mediterranean Sea in an ensemble of coupled atmosphere–ocean regional climate models. *Clim. Dynam.* 39, 1859—1884. doi: 10.1007/s00382-011-1261-4

Estournel, C., Marsaleix, P., and Ulses, C. (2021). A new assessment of the circulation of Atlantic and intermediate waters in the Eastern Mediterranean. *Prog. Oceanogr.* 198, 102673. doi: 10.1016/j.pocean.2021.102673

Eusebi Borzelli, G. L., and Carniel, S. (2023). A reconciling vision of the Adriatic-Ionian Bimodal Oscillating System. *Sci. Rep.* 13, 2334. doi: 10.1038/s41598-023-29162-2

Gačić, M., Borzelli, G. L. E., Civitarese, G., Cardin, V., and Yari, S. (2010). Can internal processes sustain reversals of the ocean upper circulation? The Ionian Sea example. *Geophys. Res. Lett.* 37, 2010GL043216. doi: 10.1029/2010GL043216

Gačić, M., Civitarese, G., Miserocchi, S., Cardin, V., Crise, A., and Mauri, E. (2002). The open ocean convection in the Southern Adriatic: a controlling mechanism of the spring phytoplankton bloom. *Cont. Shelf Res.* 22, 1897–1908. doi: 10.1016/S0278-4343(02)00050-X

Gačić, M., Schroeder, K., Civitarese, G., Cosoli, S., Vetrano, A., and Eusebi Borzelli, G. L. (2013). Salinity in the Sicily Channel corroborates the role of the Adriatic–Ionian Bimodal Oscillating System (BiOS) in shaping the decadal variability of the Mediterranean overturning circulation. *Ocean Sci.* 9, 83—90. doi: 10.5194/os-9-83-2013

Giorgi, F. (2006). Climate change hot-spots. *Geophys. Res. Lett.* 33, 2006GL025734. doi: 10.1029/2006GL025734

Glamuzina, B., Vilizzi, L., Piria, M., Žuljević, A., Cetinić, A. B., Pešić, A., et al. (2024). Global warming scenarios for the eastern Adriatic Sea indicate a higher risk of invasiveness of non-native marine organisms relative to current climate conditions. *Mar. Life Sci. Technol.* 6, 143—154. doi: 10.1007/s42995-023-00196-9

Good, S. A., Martin, M. J., and Rayner, N. A. (2013). En4: Quality controlled ocean temperature and salinity profiles and monthly objective analyses with uncertainty estimates. *J. Geophys. Res. Oceans* 118, 6704—6716. doi: 10.1002/2013JC009067

Gouretski, V. (2018). World Ocean Circulation Experiment – Argo global hydrographic climatology. *Ocean Sci.* 14, 1127–1146. doi: 10.5194/os-14-1127-2018

Hadfield, R. E., Wells, N. C., Josey, S. A., and Hirschi, J. J. (2007). On the accuracy of North Atlantic temperature and heat storage fields from Argo. *J. Geophys. Res. Oceans* 112, C01009. doi: 10.1029/2006JC003825

Hersbach, H., Bell, B., Berrisford, P., Biavati, G., Horányi, A., Muñoz Sabater, J., et al. (2023). ERA5 hourly data on single levels from 1940 to present. *Copernicus Climate Change Service (C3S) Climate Data Store (CDS)*. doi: 10.24381/cds.adbb2d47

Josey, S. A., and Schroeder, K. (2023). Declining winter heat loss threatens continuing ocean convection at a Mediterranean dense water formation site. *Environ. Res. Letter* 18, 024005. doi: 10.1088/1748-9326/aca9e4

Klein, B., Roether, W., Manca, B. B., Bregant, D., Beitzel, V., Kovacevic, V., et al. (1999). The large deep water transient in the Eastern Mediterranean. *Deep Sea Res. Part I: Oceanogr. Res. Papers* 46, 371—414. doi: 10.1016/S0967-0637(98)00075-2

Kotta, D., and Kitsiou, D. (2019). Chlorophyll in the Eastern Mediterranean Sea: Correlations with environmental factors and trends. *Environment* 6. doi: 10.3390/environments6080098

Kubin, E., Menna, M., Mauri, E., Notarstefano, G., Mieruch, S., and Poulain, P.-M. (2023). Heat content and temperature trends in the Mediterranean Sea as derived from Argo float data. *Front. Mar. Sci.* 10. doi: 10.3389/fmars.2023.1271638

Lavigne, H., Civitarese, G., Gačić, M., and D'Ortenzio, F. (2018). Impact of decadal reversals of the north Ionian circulation on phytoplankton phenology. *Biogeosciences* 15, 4431—4445. doi: 10.5194/bg-15-4431-2018

Li, P., and Tanhua, T. (2020). Recent changes in deep ventilation of the Mediterranean Sea; evidence from long-term transient tracer observations. *Front. Mar. Sci.* 7. doi: 10.3389/fmars.2020.00594

Liu, C., Liang, X., Ponte, R. M., and Chambers, D. P. (2024). "Salty drift" of Argo floats affects the gridded ocean salinity products. *J. Geophys. Res. Oceans* 129, e2023JC020871. doi: 10.1029/2023JC020871

Manca, B., Burca, M., Giorgetti, A., Coatanoan, C., Garcia, M.-J., and Iona, A. (2004). Physical and biochemical averaged vertical profiles in the Mediterranean regions: an important tool to trace the climatology of water masses and to validate incoming data from operational oceanography. *J. Mar. Syst.* 48, 83—116. doi: 10.1016/j.jmarsys.2003.11.025

Margirier, F., Testor, P., Heslop, E., Mallil, K., Bosse, A., Houpert, L., et al. (2020). Abrupt warming and salinification of intermediate waters interplays with decline of deep convection in the Northwestern Mediterranean Sea. *Sci. Rep.* 10, 20923. doi: 10.1038/s41598-020-77859-5

Martellucci, R., Mendoza, F. P. D., Menna, M., Pirro, A., Reale, M., Gačić, M., et al. (2025). A multi observation analysis of the 2017 dense water formation events: climate change, bottom density currents and Adriatic-Ionian Sea circulation (Mediterranean Sea). *J. Geophys. Res. Oceans* 130, e2024JC022306. doi: 10.1029/2024JC022306

Meli, M. (2024). The potential recording of North Ionian Gyre's reversals as a decadal signal in sea level during the instrumental period. *Sci. Rep.* 14, 4907. doi: 10.1038/s41598-024-55579-4

Menna, M., Gerin, R., Notarstefano, G., Mauri, E., Bussani, A., Pacciaroni, M., et al. (2021). On the circulation and thermohaline properties of the Eastern Mediterranean Sea. *Front. Mar. Sci.* 8. doi: 10.3389/fmars.2021.671469

Menna, M., Suárez, N. C. R., Civitarese, G., Gačić, M., Rubino, A., and Poulain, P.-M. (2019). Decadal variations of circulation in the central Mediterranean and its interactions with mesoscale gyres. *Deep-Sea Res. Part II: Topical Stud. Oceanogr.* 164, 14–24. doi: 10.1016/j.dsr2.2019.02.004

Mihanović, H., Vilibić, I., Dunić, N., and Šepić, J. (2015). Mapping of decadal middle Adriatic oceanographic variability and its relation to the BiOS regime. *J. Geophys. Res. Oceans* 120, 5615—5630. doi: 10.1002/2015JC010725

Ozer, T., Gertman, I., Kress, N., Silverman, J., and Herut, B. (2017). Interannual thermohaline, (1979–2014) and nutrient, (2002–2014) dynamics in the Levantine surface and intermediate water masses, SE Mediterranean Sea. *Global Planet. Change* 151, 60–67. doi: 10.1016/j.gloplacha.2016.04.001

Ozer, T., Rahav, E., Gertman, I., Sisma-Ventura, G., Silverman, J., and Herut, B. (2022). Relationship between thermohaline and biochemical patterns in the Levantine upper and intermediate water masses, Southeastern Mediterranean Sea, (2013–2021). *Front. Mar. Sci.* 9. doi: 10.3389/fmars.2022.958924

Parras-Berrocal, I. M., Waldman, R., Sevault, F., Somot, S., Gonzalez, N., Ahrens, B., et al. (2024). Response of the Mediterranean Sea surface circulation at various global warming levels: A multi-model approach. *Geophys. Res. Lett.* 51, e2024GL111695. doi: 10.1029/2024GL111695

Patti, B., Torri, M., Placenti, F., and Cuttitta, A. (2025). Impact of the Adriatic–Ionian Bimodal Oscillating System (BiOS) on the biodiversity patterns of the larval fish community in the north-eastern sector of the Strait of Sicily (central Mediterranean, Malta Channel). *Front. Earth Sci.* 13. doi: 10.3389/feart.2025.1531521

Pinardi, N., Cessi, P., Borile, F., and Wolfe, C. L. P. (2019). The Mediterranean Sea overturning circulation. *J. Phys. Oceanogr.* 49, 1699–1721. doi: 10.1175/JPO-D-18-0254.1

Placenti, F., Torri, M., Pessini, F., Patti, B., Tancredi, V., Cuttitta, A., et al. (2022). Hydrological and biogeochemical patterns in the Sicily Channel: New insights from the last decade, (2010–2020). *Front. Mar. Sci.* 9. doi: 10.3389/fmars.2022.733540

Potiris, M., Mamoutos, I. G., Tragou, E., Zervakis, V., Kassis, D., and Ballas, D. (2024a). Dense water formation in the north–central Aegean Sea during winter 2021–2022. *J. Mar. Sci. Eng.* 12, 221. doi: 10.3390/jmse12020221

Potiris, M., Mamoutos, I. G., Tragou, E., Zervakis, V., Kassis, D., and Ballas, D. (2024b). Dense water formation variability in the Aegean Sea from 1947 to 2023. *Oceans* 5, 611—636. doi: 10.3390/oceans5030035

Raicich, F., Malačič, V., Celio, M., Giaiotti, D., Cantoni, C., Colucci, R. R., et al. (2013). Extreme air-sea interactions in the Gulf of Trieste (North Adriatic) during the strong Bora event in winter 2012: Air-sea interactions in winter 2012. *J. Geophys. Res. Oceans* 118, 5238—5250. doi: 10.1002/jgrc.20398

Reale, M., Cossarini, G., Lazzari, P., Lovato, T., Bolzon, G., Masina, S., et al. (2022). Acidification, deoxygenation, and nutrient and biomass declines in a warming Mediterranean Sea. *Biogeosciences* 19, 4035—4065. doi: 10.5194/bg-19-4035-2022

Roether, W., Klein, B., Beitzel, V., and Manca, B. B. (1998). Property distributions and transient-tracer ages in levantine intermediate water in the Eastern Mediterranean. *J. Mar. Syst.* 18, 71—87. doi: 10.1016/S0924-7963(98)00006-2

Roether, W., Manca, B. B., Klein, B., Bregant, D., Georgopoulos, D., Beitzel, V., et al. (1996). Recent changes in Eastern Mediterranean deep waters. *Science* 271, 333—335. doi: 10.1126/science.271.5247.333

Rubino, A., Gačić, M., Bensi, M., Kovačević, V., Malačič, V., Menna, M., et al. (2020). Experimental evidence of long-term oceanic circulation reversals without wind influence in the North Ionian Sea. *Sci. Rep.* 10, 1905. doi: 10.1038/s41598-020-57862-6

Salgado-Hernanz, P., Racault, M.-F., Font-Muñoz, J., and Basterretxea, G. (2019). Trends in phytoplankton phenology in the Mediterranean Sea based on ocean-color remote sensing. *Remote Sens. Environ.* 221, 50–64. doi: 10.1016/j.rse.2018.10.036

Sampatakaki, A., Zervakis, V., Mamoutos, I., Tragou, E., Gogou, A., Triantaphyllou, M., et al. (2021). Investigation of the inherent variability of the Mediterranean Sea under contrasting extreme climatic conditions. *Front. Mar. Sci.* 8, 656737. doi: 10.3389/fmars.2021.656737

Saporta-Katz, O., Mantel, N., Liran, R., Rom-Kedar, V., and Gildor, H. (2024). Northbound transport of the Mediterranean outflow and the role of time-dependent chaotic advection. *Geophys. Res. Lett.* 51, e2023GL105662. doi: 10.1029/2023GL105662

Schlitzer, R. (2018). *Ocean data view (odv)*.

Sellschopp, J., and Álvarez, A. (2003). Dense low-salinity outflow from the Adriatic Sea under mild, (2001) and strong, (1999) winter conditions. *J. Geophys. Res.* 108, 8104. doi: 10.1029/2002JC001562

Sisma-Ventura, G., Kress, N., Silverman, J., Gertner, Y., Ozer, T., Biton, E., et al. (2021). Post-Eastern Mediterranean transient oxygen decline in the deep waters of the southeast Mediterranean Sea supports weakening of ventilation rates. *Front. Mar. Sci.* 7. doi: 10.3389/fmars.2020.598686

Skliris, N., Marsh, R., Breedon, M., and Josey, S. A. (2024). Accelerated warming and salinification of the Mediterranean Sea: implications for dense water formation. *J. Mar. Sci. Eng.* 13, 25. doi: 10.3390/jmse13010025

Soto-Navarro, J., Jordá, G., Amores, A., Cabos, W., Somot, S., Sevault, F., et al. (2020). Evolution of Mediterranean Sea water properties under climate change scenarios in the Med-CORDEX ensemble. *Clim. Dynam.* 54, 2135—2165. doi: 10.1007/s00382-019-05105-4

Taillandier, V., Lherminier, P., Grob, C., D'Ortenzio, F., Pastres, R., Morin, P., et al. (2022). Decadal variability of the Mediterranean Sea circulation and heat budget from a multi-decade boundary value problem approach. *J. Geophys. Res. Oceans* 127, e2021JC01750. doi: 10.1029/2021JC01750

Terzić, E., Cardin, V., Le Meur, J., Dunić, N., Vodopivec, M., and Vilibić, I. (2025a). Unprecedented warming and salinization observed in the deep Adriatic. *Limnol. Oceanogr. Lett.* 10 (6), 888-898. doi: 10.1002/lol2.70051

Terzić, E., Gardiol, C., and Vilibić, I. (2025b). Surface saline lakes in the Mediterranean Sea. *Ocean Sci.* 21, 1441—1459. doi: 10.5194/os-21-1441-2025

Vecchioni, G., Cessi, P., Pinardi, N., Rousselet, L., and Trotta, F. (2023). A lagrangian estimate of the Mediterranean outflow's origin. *Geophys. Res. Lett.* 50, e2023GL103699. doi: 10.1029/2023GL103699

Velaoras, D., Krokos, G., Nittis, K., and Theocharis, A. (2014). Dense intermediate water outflow from the Cretan Sea: A salinity driven, recurrent phenomenon, connected to thermohaline circulation changes. *J. Geophys. Res. Oceans* 119, 4797—4820. doi: 10.1002/2014JC009937

Wong, A. P. S., Gilson, J., and Cabanes, C. (2023). Argo salinity: bias and uncertainty evaluation. *Earth Syst. Sci. Data* 15, 383—393. doi: 10.5194/essd-15-383-2023

Zodiatis, G., Brenner, S., Gertman, I., Ozer, T., Simoncelli, S., Ioannou, M., et al. (2023). Twenty years of *in-situ* monitoring in the south-Eastern Mediterranean Levantine basin: Basic elements of the thermohaline structure and of the mesoscale circulation during 1995-2015. *Front. Mar. Sci.* 9. doi: 10.3389/fmars.2022.10745